

# NJC

Accepted Manuscript



This article can be cited before page numbers have been issued, to do this please use: A. Tillo, D. T. Mlynczyk, L. Popena, B. Wicher, M. Kryjewski, W. Szczolko, S. Jurga, J. Mielcarek, M. Gdaniec, T. Goslinski and E. Tykarska, *New J. Chem.*, 2017, DOI: 10.1039/C6NJ03886G.



This is an Accepted Manuscript, which has been through the Royal Society of Chemistry peer review process and has been accepted for publication.

Accepted Manuscripts are published online shortly after acceptance, before technical editing, formatting and proof reading. Using this free service, authors can make their results available to the community, in citable form, before we publish the edited article. We will replace this Accepted Manuscript with the edited and formatted Advance Article as soon as it is available.

You can find more information about Accepted Manuscripts in the [author guidelines](#).

Please note that technical editing may introduce minor changes to the text and/or graphics, which may alter content. The journal's standard [Terms & Conditions](#) and the ethical guidelines, outlined in our [author and reviewer resource centre](#), still apply. In no event shall the Royal Society of Chemistry be held responsible for any errors or omissions in this Accepted Manuscript or any consequences arising from the use of any information it contains.



## Journal Name

## ARTICLE

## Synthesis and singlet oxygen generation of pyrazinoporphyrazines containing dendrimeric aryl substituents

Adam Tillo<sup>a</sup>, Dariusz T. Mlynarczyk<sup>a</sup>, Lukasz Popenda<sup>b</sup>, Barbara Wicher<sup>a</sup>, Michal Kryjewski<sup>\*c</sup>, Wojciech Szczolko<sup>a</sup>, Stefan Jurga<sup>b,d</sup>, Jadwiga Mielcarek<sup>c</sup>, Maria Gdaniec<sup>e</sup>, Tomasz Goslinski<sup>a</sup>, Ewa Tykarska<sup>\*a</sup>

Received 00th January 20xx,  
Accepted 00th January 20xx

DOI: 10.1039/x0xx00000x

www.rsc.org/

Pyrazinoporphyrazines and tribenzopyrazinoporphyrazines were synthesized and studied towards their potential applications in photodynamic therapy. The macrocycles were obtained via Linstead macrocyclization with good yields. The expansion of the porphyrazine periphery with hyperbranched aryl substituents was beneficial in terms of purification and isolation of compounds, effectively hampering their aggregation tendency in different concentrations. The obtained macrocycles were assessed for their singlet oxygen generation quantum yields and revealed far better efficacies for tribenzopyrazinoporphyrazines than pyrazinoporphyrazines. Comparison of crystal packing of two 2,3-dicyanopyrazine derivatives revealed that recurring motif of supramolecular architecture is a dimer formed by  $\pi$ - $\pi$  stacking interactions between aromatic pyrazine and phenyl rings of the inversion center related molecules.

### Introduction

Porphyrazines (Pzs) are synthetic macrocycles, which are analogues of naturally occurring porphyrinoids like heme or chlorophyll. In the Pz macrocycle the pyrrole rings are bound together by aza bridges, in contrast to methine groups found in porphyrins.<sup>1</sup>

Benzene-fused derivatives of porphyrazines - phthalocyanines have been used for decades as dyes and pigments in textile and paper industry.<sup>2</sup> Recently, they have been extensively studied for their possible use in a broad range of both technical and medical applications.<sup>2,3</sup> Some of the modern research areas for their further use are industrial catalytic systems, semiconductors, chemical sensors, materials for electrophotography, and advanced functional materials.<sup>2,4,5</sup> Peripherally substituted tetrapyrrolyl porphyrazines have become one of the most easily accessible phthalocyanine analogues.<sup>6</sup>

Porphyrazines raise a lot of interest for their possible use in biomedical sciences. Their unique spectral and

physicochemical properties make them possible candidates for photosensitizers in photodynamic therapy (PDT),<sup>7-9</sup> radiation therapy,<sup>10</sup> boron neutron capture therapy and in bioimaging.<sup>3</sup> In PDT, photosensitizer is delivered to the tumor tissue, where upon irradiation with light of an appropriate wavelength it generates reactive oxygen species, including singlet oxygen. These species have the ability to kill tumor cells leading further to their necrosis or apoptosis. Currently used photosensitizers are still far from being ideal. Improvement in their biophysical properties, while maintaining high singlet oxygen generation yield is still a subject of research.<sup>8</sup> One of the main factors, hampering effective biological activity of porphyrinoids is their poor solubility in water and tendency to form aggregates resulting from high molecular mass and  $\pi$ -bond stacking interactions. Aggregation tendency can lead to efficient non-radiative energy relaxation, thereby reducing macrocycles triplet-state population and consequently significantly decreasing their photosensitizing efficacy.<sup>11</sup>

Pz molecule can be modified by peripheral functionalization and/or insertion of a metal ion into the macrocycle core. These structural changes can effectively improve the macrocycle solubility, as well as prevent the aggregation of its molecules.<sup>12</sup> One of the most common synthetic routes to octakis-functionalized porphyrazines is the cyclization of the functionalized maleonitrile derivatives in the presence of magnesium alkoxide (Linstead macrocyclization).<sup>13</sup> Various dicyano derivatives of N-heterocycles themselves have been a subject of interest for chemical industry, as well as food, agricultural and medicinal chemistry.<sup>14,15</sup> 2,3-Dicyanopyrazine derivatives are most commonly used substrates for pyrazinoporphyrazine synthesis.<sup>6</sup> 2,3-Dicyanopyrazine heterocycle comprises two strong electron withdrawing cyano

<sup>a</sup> Department of Chemical Technology of Drugs, Poznan University of Medical Sciences, Grunwaldzka 6, 60-780 Poznan, Poland, E-mail: etykarsk@ump.edu.pl

<sup>b</sup> NanoBioMedical Centre, Adam Mickiewicz University, Umultowska 85, 61-614 Poznan, Poland

<sup>c</sup> Department of Inorganic and Analytical Chemistry, Poznan University of Medical Sciences, Grunwaldzka 6, 60-780 Poznan, Poland, E-mail: mkryjewski@ump.edu.pl

<sup>d</sup> Department of Macromolecular Physics, Faculty of Physics, Adam Mickiewicz University, Umultowska 85, 61-614 Poznan, Poland

<sup>e</sup> Faculty of Chemistry, Adam Mickiewicz University, Umultowska 89b, 61-614 Poznan, Poland

† Electronic Supplementary Information (ESI) available: Additional experimental details and spectral data. See DOI: 10.1039/x0xx00000x

## ARTICLE

## Journal Name

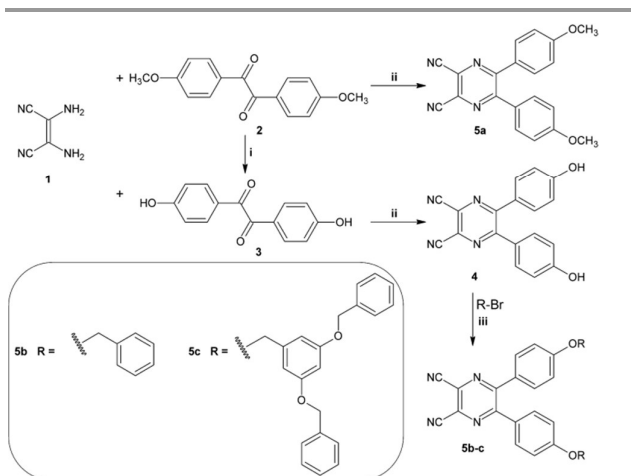
groups, which results in its specific properties. Despite the small chromophoric system of dicyanopyrazine, it shows strong fluorescence, even in the solid state<sup>15</sup>. Highly functionalized 2,3-dicyanopyrazine derivatives have been recently extensively studied for their possible use as a functional dyes, electroluminescence materials and amorphous molecular glass.<sup>15,16</sup> A wide range of aminoporphyrazine derivatives, possessing heterocyclic diazepine,<sup>17,18</sup> pyrrole,<sup>19,20</sup> or pyrazine rings<sup>21,22</sup> have been synthesized. The nature of the substituent strongly influenced electronic and optical properties of the macrocycle. Moreover, tetrapyrazinoporphyrazines have been studied as potential photosensitizers in PDT.<sup>23</sup>

In the present study, pyrazinoporphyrazines and tribenzopyrazinoporphyrazines were designed and studied towards their potential application in photodynamic therapy. The expansion of the porphyrazine periphery with hyperbranched aryl substituents was found to be beneficial as it ensures easier purification and prevents its aggregation. The effect of symmetry and peripheral expansion on singlet oxygen generation yields and aggregation was extensively studied in both macrocycle types.

## Results and discussion

### Molecular design and synthesis

The aim of our study was to design novel pyrazinoporphyrazines with hyperbranched peripheral substituents. We have synthesized, isolated and characterized novel porphyrazines containing annulated pyrazine rings. The peripheries of the obtained macrocycles were equipped with dendritic wedges and represent both pyrazinoporphyrazines (A<sub>4</sub>) as well as tribenzopyrazinoporphyrazines (A<sub>3</sub>B).

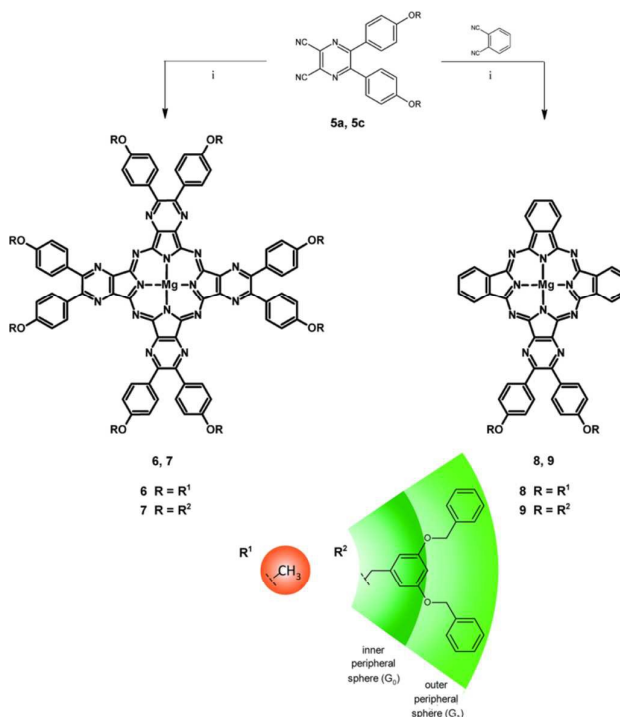


**Scheme 1.** Reagents and conditions: (i) pyridine hydrochloride, 220 °C, 1.5 h; (ii) *p*-toluenesulfonic acid, CH<sub>3</sub>OH, reflux, 18 h; (iii) K<sub>2</sub>CO<sub>3</sub>, DMF, 60 °C, 18 h.

Compounds **4** and **5a** have been previously synthesized and characterized by Cristiano et al.<sup>15</sup> Diaminomaleonitrile **1** was subjected to condensation reaction with anisole **2** to give **5a**

(Scheme 1). The use of pyridine hydrochloride<sup>24</sup> was found to be more efficient (90% yield) for demethylation of anisole **2** to dihydroxy derivative **3**, comparing to the originally published procedure with aqueous HBr (69% yield).<sup>15</sup> Alkylation reaction of 2,3-dicyanopyrazine derivative **4** with benzyl bromide and 3,5-bis(benzyloxy)benzyl bromide led to compounds **5b** and **5c**, respectively. Known alkylating agent, 3,5-bis(benzyloxy)benzyl bromide was prepared in a four step process. Briefly, 3,5-dihydroxybenzoic acid was converted to methyl ester<sup>25</sup>, which was subsequently alkylated with benzyl bromide, leading to methyl 3,5-bis(benzyloxy)benzoate.<sup>26,27</sup> Obtained ester was reduced to alcohol<sup>28</sup> and converted to bromide following the Hawker procedure.<sup>29</sup>

Dicyanopyrazine derivatives **5a-c** were applied in the Lindsey macrocyclization reaction, employing magnesium *n*-butanolate solution in *n*-butanol<sup>13</sup> towards symmetrical macrocycle derivatives (Scheme 2). In addition, in analogous conditions, 2,3-dicyanopyrazines **5a-c** and excess of 1,2-dicyanobenzene were subjected to macrocyclization reaction towards tribenzoporphyrazine derivatives.<sup>30</sup> Massive aggregation of products obtained in macrocyclization reactions in which 2,3-dicyanopyrazine derivative **5b** was used, hampered their effective isolation as pure products (see discussion and characterization in Supplementary data). When **5a** and **5c** were used as substrates, it was possible to isolate with good yields symmetrical porphyrazine derivatives **6**, **7** as well as tribenzoporphyrazine derivatives **8** and **9**.



**Scheme 2.** Synthetic route leading to porphyrazines **6-9**. Reagents and conditions: (i) Mg(*n*-OBu)<sub>2</sub>, *n*-BuOH, reflux, 20 h.

Porphyrazines **6-9** were isolated and characterized by means of HRMS spectrometry and studied in detail by NMR



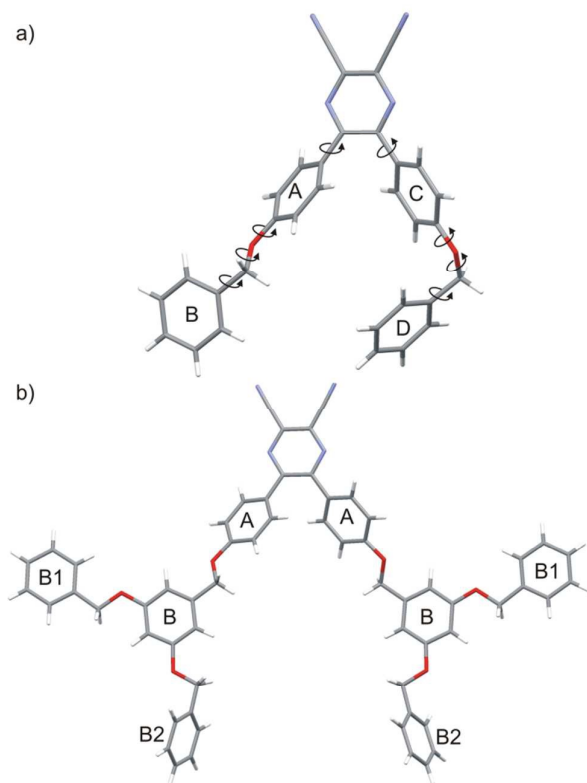
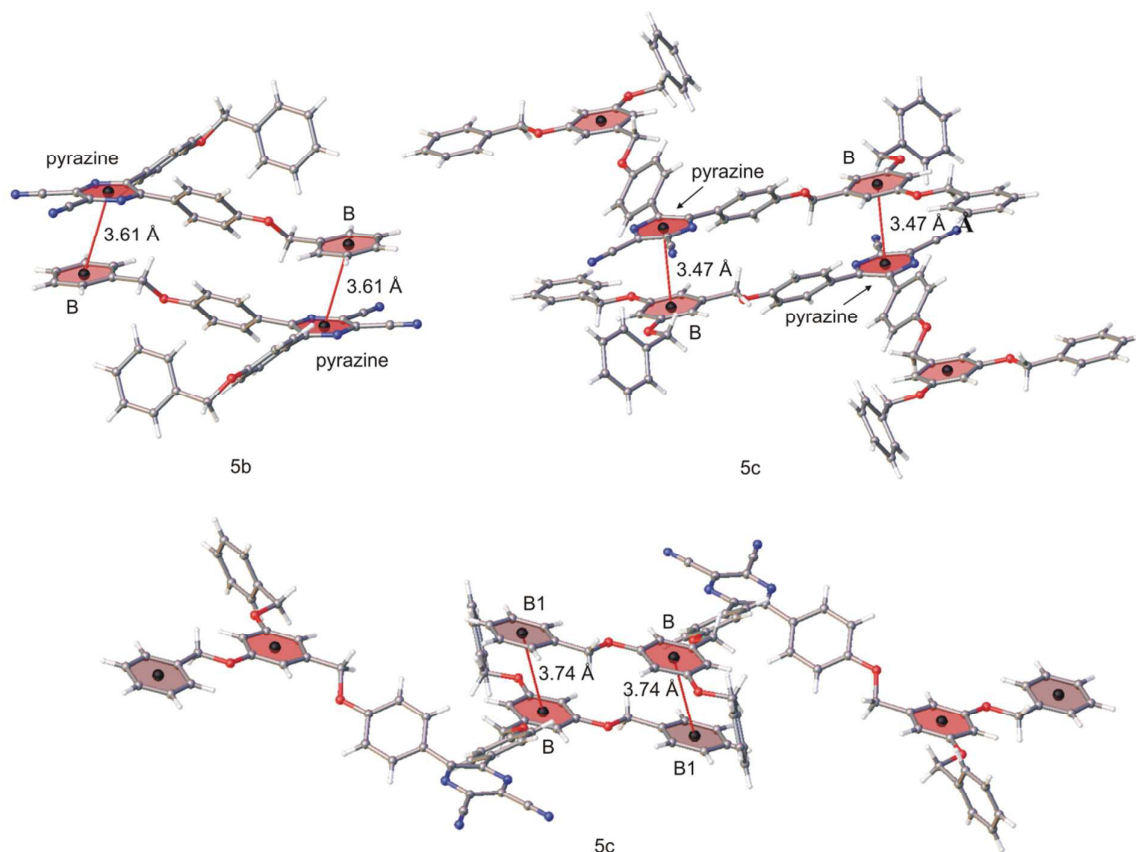


Fig. 2. Caped-stick representation of **5b** and **5c**.

twofold symmetry axis. The asymmetric unit consist of one half of the dicyanopyrazine derivative and one dichloromethane molecule (Fig. S25).

In **5b** the two 4-(benzyloxy)phenyl substituents adopt different conformations resulting from the rotation about single bonds presented in Fig. 2a. The inner A and C rings are twisted by  $45.0(1)^\circ$  and  $39.1(1)^\circ$ , respectively, in the same direction against planar pyrazine ring. Similar twist of the benzene rings was observed in 2,3-dicyano-5,6-bis(4-methoxyphenyl)pyrazine.<sup>15</sup> The  $-O-CH_2-$  groups bridging the inner and the outer benzene rings are in *trans* and *gauche* conformations (Table S8). Thus one of the benzyloxyphenyl branches adopts elongated and the other one sharply bent shapes. The pyrazine and the B rings (Fig. 2a) are oriented nearly parallel [the dihedral angle  $6.24(8)^\circ$ ] (Table S9).

In the more branched dicyanopyrazine derivative **5c** (Fig. 2b), the conformation of a zero-generation ( $G_0$ ) branch of substituted 4-(benzyloxy)phenyl moiety (ring A-O- $CH_2$ -ring B) is similar to the corresponding group of **5b**. The dihedral angles between the best planes of the pyrazine and ring A, and pyrazine and ring B are  $39.7(1)^\circ$  and  $0.6(2)^\circ$ , respectively. The  $G_1$  branches of 4-[3,5-bis(benzyloxy)benzyloxy]phenyl substituent also have the  $-O-CH_2-$  groups in *trans* conformation, however, they differ in the rotation of the terminal phenyl group about a single C-C bond (Table S8). The terminal B1 phenyl group is virtually parallel and coplanar with B ring [dihedral angle  $3.5(2)^\circ$ ] and parallel with the pyrazine ring [dihedral angle  $3.7(2)^\circ$ ], whereas the ring B2 is strongly twisted (ca.  $68^\circ$ , Table S9).



**Fig. 3.**  $\pi$ - $\pi$  stacking interactions between the pyrazine ring and the phenyl group B (top) and two phenyl groups B and B1 (bottom) in **5b** and **5c**. Lines connecting centroids are shown in red.

Parallel arrangement of some of the aromatic rings within the dicyanopyrazine derivative molecules (Table S9) is related to the molecular self-assembly in the crystals of **5b** and **5c**. In the absence of other functional groups able to form stronger intermolecular interactions only weak forces govern crystal packing of the analyzed compounds. In both crystals the dimers are formed by  $\pi$ - $\pi$  stacking interactions between the pyrazine and B rings of the inversion center related molecules (Fig. 3 top). The distances between the ring centroids are 3.61 Å in **5b** and 3.47 Å in **5c**. In **5b** the dimers further interact *via* C-H $\cdots$ O and C-H $\cdots$ N weak hydrogen bonds (Fig. S26, Table S10). In **5c**, the centrosymmetric dimers form larger 3D aggregates via  $\pi$ - $\pi$  stacking interactions between the virtually coplanar B and B1 rings (centroid $\cdots$ centroid distance 3.74 Å) (Fig. 3 bottom). The 3D network of **5c** contains centrosymmetric voids occupied by two dichloromethane molecules.

#### Aggregation studies

The aggregation tendency of the obtained porphyrazines was checked in DMF and DMSO as solvents, as aggregation may decrease singlet oxygen quantum yields and fluorescence yields. Absorbance of a series of solutions with increasing concentrations of porphyrazine were measured. Subsequently, absorbance - concentration graphs were plotted in order to

assess their consistence with the Lambert-Beer law. For the macrocycles bearing smaller peripheral substituents (**6**, **8**), the obtained plots significantly deviated from linearity, what indicates their tendency to aggregation (Fig. 4, Tables S11, S12). Our visual observations indicate that porphyrazines bearing methoxy groups (**6**, **8**) quickly form aggregates in concentrated solutions (Fig. 5). Expanding the macrocycle core with polyaryl substituents seem to be an effective way to prevent its aggregation. For the macrocycles **7** and **9** stable concentrated solutions could be prepared.

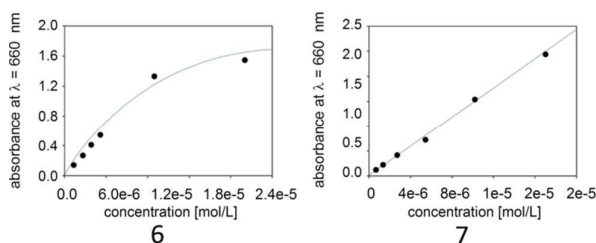


**Fig. 4.** Absorbance - concentration graphs of porphyrazines **6** and **7** in DMF.



Fig. 5. Comparison of  $2 \cdot 10^{-4}$  mol/L dichloromethane solutions of methoxy (**6**) and polyaryl (**7**) substituted porphyrazines after 40 min at ambient temperature.

#### Absorption and fluorescence studies

Porphyrazines researched in our study have the magnesium(II) ion in the central cavity. The UV-Vis spectra were analyzed taking into account the effects of the peripheral groups and symmetry of the macrocycles. Absorbance maxima (Table 1) for the A4 macrocycles **6** and **7** correspond well with published data<sup>32</sup>;  $\lambda_{\text{max}} = 659$  nm has been reported for magnesium pyrazinoporphyrazine peripherally substituted with phenyl moieties. For the symmetric porphyrazine **7** an intensive absorption band (beta-band), followed by a weaker one (alpha-band) was observed in the Q-band region. In the UV-Vis spectrum of unsymmetrical porphyrazine **9** the main band accompanied by two smaller alpha-bands was found. Introduction of the asymmetry factor to the macrocycle resulted in approximate 20 nm shifting of the absorption band towards the red (Fig. 6). Q-Band of the A3B-type porphyrazines **8** and **9** was broadened in comparison to the A4-type, which is typical for A3B porphyrazines and phthalocyanines<sup>33</sup>, however no splitting of the Q-band was observed. Our studies did not show any significant correlations between the size of peripheral side-chains present in studied compounds and their UV-Vis absorption maxima.

Fluorescence studies were conducted using zinc(II) phthalocyanine as a reference of known values<sup>34</sup> revealed low

to moderate values of fluorescence quantum yields, highest for compound **9**, and lowest for **8** (Table 1). These values are significantly lower than  $\Phi_F = 0.50$  (in pyridine), which has been previously reported by Morkved et al.<sup>32</sup> for magnesium pyrazinoporphyrazine peripherally substituted with phenyl moieties. Excitation spectra superimpose well with absorbance plots (Fig. S39-42). The Stokes shifts are minor, which confirms a small difference between geometry of the molecule in its ground and singlet  $S_1$  state. No emissions from higher singlet states were observed.

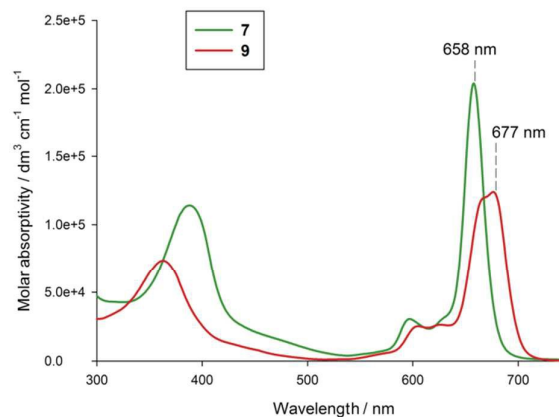


Fig. 6. UV-Vis spectra of symmetrical A<sub>4</sub> **7** (green) and A<sub>3</sub>B type **9** (red) porphyrazines in DMF.

#### Singlet oxygen generation

Effective singlet oxygen generation is a key feature of a successful PDT photosensitizer. In our studies, the designed macrocycles were assessed for their singlet oxygen generation quantum yields in DMF and DMSO, according to a previously described literature procedure.<sup>35-37</sup> The comparative method was used, employing 1,3-diphenylisobenzofuran (DPBF) as a singlet oxygen chemical quencher and zinc(II) phthalocyanine (ZnPc) as a reference (quantum yields 0.56 and 0.67 in DMF and DMSO, respectively).<sup>34,37</sup> The prepared solutions of the macrocycle and DPBF were exposed to the monochromatic light of the wavelength adjusted to the maximum absorbance of the macrocycle Q-band. The decrease of the DPBF concentration was determined by measurement of its absorption maximum at 417 nm (Fig. 7).

Comparison of DPBF oxidation kinetic parameters of porphyrazines **6-9** and ZnPc allowed calculation of the singlet oxygen generation yield (Table 1).

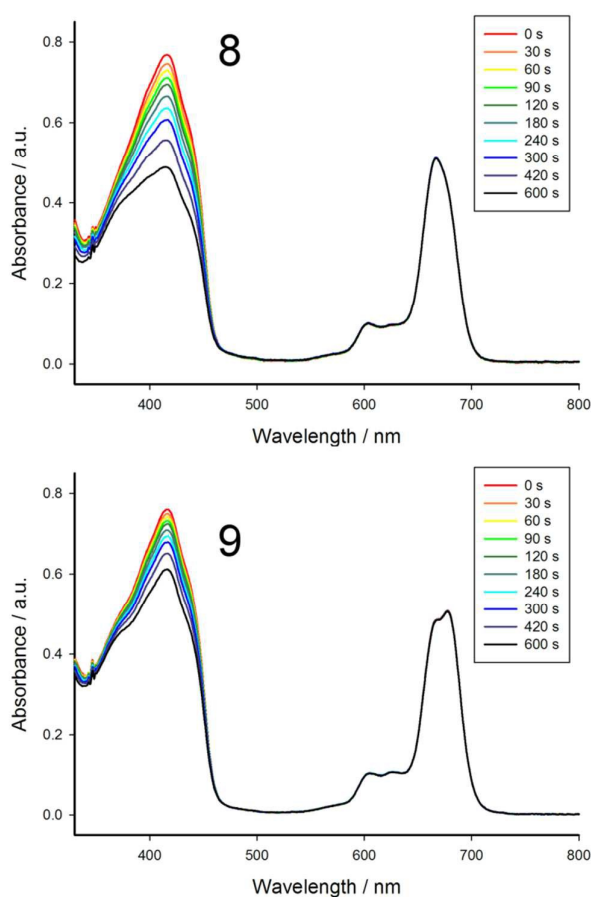
## Journal Name

## ARTICLE

**Table 1.** Singlet oxygen generation and fluorescence quantum yields of porphyrazines 6-9.

Pz	Absorbance maximum at Q-band $\lambda_{\text{max}}$ [nm]		Fluorescence maximum $\lambda_{\text{f}}$ [nm]		Fluorescence quantum yields $\Phi_{\text{f}}$		Singlet oxygen generation quantum yields $\Phi_{\Delta}$	
	DMF	DMSO	DMF	DMSO	DMF	DMSO	DMF	DMSO
6	660	658	662	664	0.07	0.26	0.04	0.07
7	658	658	662	665	0.11	0.27	0.04	0.08
8	666	667	676	678	0.07	0.02	0.22	0.26
9	677	676	677	680	0.18	0.29	0.09	0.13

For the symmetrical porphyrazines **6**, **7** low quantum yields (0.04-0.08) of singlet oxygen generation were measured. However, improved values were obtained by implementing the attribute of asymmetry to the photosensitizer. Tribenzopyrazinoporphyrazines **8**, **9** exhibited low to moderate singlet oxygen generating yields (0.09-0.26). The highest singlet oxygen generation was recorded for the methoxy-substituted A3B porphyrazine **8**. This observation is in contrast to our previous studies performed for phthalocyanines,<sup>38</sup> where introduction of dendrimeric moieties increased singlet oxygen quantum yields. However, this is consistent with very low fluorescence quantum yields measured for this compound. Value of  $\Phi_{\Delta} = 0.249$  has been reported for previously mentioned magnesium pyrazinoporphyrazine peripherally substituted with phenyl moieties.<sup>32</sup> This may be attributed to the influence of the solvent, as pyridine is known to coordinate central metal ion and prevent aggregation.

**Fig. 7.** Changes in the UV-Vis spectra of solutions of DPBF and porphyrazines **8** and **9** (in DMSO) during irradiation.**Conclusions**

Novel symmetrical ( $A_4$ ) as well as asymmetric ( $A_3B$  type) porphyrazines structures were obtained. The macrocycles were obtained in good yields, provided easy purification method and did not decompose during their prolonged storage. The compounds were studied towards key features

aiming for their use in photodynamic therapy. Expansion of the porphyrazine periphery with aryl substituents was intended to prevent the aggregation tendency, a common drawback of macrocyclic photosensitizers. Obtained porphyrazines were subsequently assessed for their singlet oxygen generation quantum yields.

In the crystalline state,  $G_0$  branches of **5c** adopt a conformation similar to that of the 4-(benzyloxy)phenyl substituent of **5b** having the terminal phenyl ring parallel with the pyrazine ring. This arrangement of the aromatic rings facilitates  $\pi$ - $\pi$  stacking interactions leading to the formation of centrosymmetric dimers that are a common supramolecular motif for **5c** and **5b**.

Far better singlet oxygen generation efficacies for the tribenzoporphyrazines were found. Our laboratory observations indicate that all of the synthesized methoxy- and benzyloxy-substituted macrocycles strongly aggregate and they are hardly soluble in any common organic solvents. As previously reported,<sup>38</sup> attachment of the dendritic-like substituents can successfully improve the solubility of porphyrazines and phthalocyanines. Despite large structures of molecules and strong hydrophobic nature, solutions of porphyrazines **7** and **9** remained stable in broad concentration range. Similarly, introduction of polyaryl substituents improves fluorescence quantum yields.

Tribenzoporphyrazine **9** with its dendrimeric periphery shows promising properties as a potential PDT photosensitizer, considering its solubility, the lack of aggregation and moderate singlet oxygen generation yield. Further functionalization of the peripheral side chain could bring the photosensitizer well soluble in polar solvents.

## Experimental

### Chemicals and instrumentation

All reactions were conducted in oven dried glassware under argon atmosphere using Radleys Heat-On heating system. All solvents were rotary evaporated at or below 60 °C under reduced pressure. All solvents and reagents were obtained from commercial suppliers and used without further purification, unless otherwise stated. Flash column chromatography was carried out on Merck silica gel 60, particle size 0.040 – 0.063 mm, Merck aluminum oxide 90, particle size 0.063 – 0.2 mm, and reverse phase Fluka C18 silica gel 90. Thin layer chromatography (TLC) was performed on Merck Kieselgel 60 F 254 plates or Fluka aluminum oxide TLC cards, 60 Å pore diameter and visualized with UV ( $\lambda_{\max}$  = 254 or 365 nm). UV-Vis spectra were recorded on a Hitachi UV/VIS U-1900 and Shimadzu PC-160 spectrophotometers. The NMR spectra were acquired on Agilent DD2 800 spectrometer operating at resonance frequencies of 799.903 and 201.146 MHz for  $^1\text{H}$  and  $^{13}\text{C}$ , respectively. Chemical shifts ( $\delta$ ) are quoted in parts per million (ppm) and are referred to a residual solvent peak. Coupling constants (J) are quoted in hertz (Hz). The abbreviations s, bs, d, t, and m refer to singlet, broad singlet, doublet, triplet, and multiplet, respectively.  $^1\text{H}$  and  $^{13}\text{C}$

NMR resonances were unambiguously assigned on the basis of  $^1\text{H}$ - $^1\text{H}$  COSY,  $^1\text{H}$ - $^{13}\text{C}$  HSQC and  $^1\text{H}$ - $^{13}\text{C}$  HMBC spectra. All NMR experiments were carried out at 298 K, except for samples **7** and **8** where data were collected at 353 K. Mass spectra (ES, MALDI TOF, HRMS) were carried out by the Advanced Chemical Equipment and Instrumentation Facility at the Faculty of Chemistry and the Wielkopolska Center for Advanced Technologies at Adam Mickiewicz University in Poznan. Melting points were obtained on a "Stuart" Bibby apparatus and are uncorrected.

### Synthesis

Compounds **4** and **5a** have been previously synthesized and characterized by Cristiano et al.<sup>15</sup>

#### 2,3-Dicyano-5,6-bis-[4-(benzyloxy)phenyl]pyrazine (**5b**)

Compound **4** (0.720 g, 2.25 mmol) and  $\text{K}_2\text{CO}_3$  (0.930 g, 6.75 mmol) were heated in DMF (20 mL) at 60 °C for 30 min. Afterwards, benzyl bromide (0.8 mL, 6.75 mmol) was added and the reaction mixture was vigorously stirred at 60 °C for 18 h. Next, the reaction mixture was cooled down and poured into 10% NaOH solution (100 mL). The oily precipitate was stirred for 30 min, then Celite filtered. After washing with water, the product was rinsed down with acetone. The obtained solution was concentrated, brine was added and mixture was extracted with  $\text{CH}_2\text{Cl}_2$  (3  $\times$  50 mL). Combined organic layers were dried with  $\text{MgSO}_4$  and vaporized. Obtained yellow oil was purified by means of column chromatography ( $\text{CH}_2\text{Cl}_2$ /n-hexane 1:5 to 1:2) to give **5b** as a yellow powder (0.320 g, 28%). Mp. 190-192 °C (AcOEt/n-hexane).  $R_f$  ( $\text{CH}_2\text{Cl}_2$ /n-hexane 1:1) 0.24.  $^1\text{H}$  NMR (800 MHz,  $\text{DMSO}-d_6$ )  $\delta$ , ppm: 7.49 (d, J = 7.5 Hz, 4H), 7.45 (d, J = 7.5 Hz, 4H), 7.40 (t, J = 7.5 Hz, 4H), 7.34 (t, J = 7.5 Hz, 2H), 7.06 (d, J = 7.0 Hz, 4H), 5.14 (s, 4H).  $^{13}\text{C}$  NMR (201 MHz,  $\text{DMSO}-d_6$ )  $\delta$ , ppm: 160.3, 153.8, 136.4, 131.3, 129.0, 128.4, 128.1, 128.0, 127.8, 115.0, 114.3, 69.4. HRMS (MALDI) Found:  $[\text{M}+\text{Na}]^+$  517.1626; molecular formula  $\text{C}_{32}\text{H}_{22}\text{N}_4\text{O}_2+\text{Na}$  requires  $[\text{M}+\text{Na}]^+$  517.1640.

#### 2,3-Dicyano-5,6-bis-[4-[3,5-bis(benzyloxy)benzyloxy]phenyl]pyrazine (**5c**)

Compound **4** (0.359 g, 1.1 mmol) and  $\text{K}_2\text{CO}_3$  (0.386 g, 2.8 mmol) were heated in DMF (8 mL) at 60 °C for 30 min. Afterwards, 3,5-bis(benzyloxy)benzyl bromide (1.1 g, 2.8 mmol) was added and the reaction mixture was vigorously stirred at 60 °C for 18 h. Next, the reaction mixture was cooled down and Celite filtrated, which was rinsed with  $\text{CH}_2\text{Cl}_2$ . The combined filtrates were evaporated to dryness with toluene. Obtained crude product was purified on silica-gel column ( $\text{CH}_2\text{Cl}_2$  to  $\text{CH}_2\text{Cl}_2$ /MeOH 20:1) to give **5c** as a yellow powder (0.850 g, 84%). Mp. 148 °C (AcOEt/2-propanol).  $R_f$  ( $\text{CH}_2\text{Cl}_2$ /n-hexane 1:1) 0.22.  $^1\text{H}$  NMR (800 MHz,  $\text{DMSO}-d_6$ )  $\delta$ , ppm: 7.49 (d, J = 7.5 Hz, 4H), 7.42 (d, J = 7.5 Hz, 8H), 7.37 (t, J = 7.5 Hz, 8H), 7.31 (m, 4H), 7.03 (d, J = 7.0 Hz, 4H), 6.70 (d, J = 2.4 Hz, 4H), 6.64 (t, J = 2.4 Hz, 2H), 5.07 (s, 8H), 5.06 (s, 4H).  $^{13}\text{C}$  NMR (201 MHz,  $\text{DMSO}-d_6$ )  $\delta$ , ppm: 160.2, 159.6, 153.8, 138.8, 136.9, 131.3, 128.9, 128.4, 128.1, 127.8, 127.7, 115.0, 114.3, 106.6, 101.3, 69.3, 69.2. HRMS (MALDI) Found:  $[\text{M}+\text{Na}]^+$  941.3280; molecular formula  $\text{C}_{60}\text{H}_{46}\text{N}_4\text{O}_6+\text{Na}$  requires  $[\text{M}+\text{Na}]^+$  941.3315.

**General procedure for preparation of tetrapyrzino porphyrazines (6 and 7)**

Symmetrical macrocyclics **6** and **7** were prepared according to classical Lindsey procedure.<sup>13</sup> Magnesium turnings (1 equiv) were refluxed in n-butanol (7 mL for each mmol of substrate) with a catalytic amount of iodine for 3 hours. After cooling down of the slurry, 2,3-dicyanopyrazine derivative was added and the mixture was refluxed for 20 hours. After cooling down, reaction mixture was sonicated and Celite filtered, which was rinsed with CH<sub>2</sub>Cl<sub>2</sub>. Filtrates were evaporated to dryness with addition of toluene, giving dark-green solid residue.

**Magnesium(II) 2,3,9,10,16,17,23,24-octakis(4-methoxyphenyl)-1,4,8,11,15,18,22,25-(octaaza)phthalocyanine (6)**

The obtained product was precipitated from CH<sub>2</sub>Cl<sub>2</sub>/n-hexane mixture. Solid precipitate was filtered on blotting paper, washed with n-hexane, CH<sub>3</sub>OH and acetone, then rinsed down with CH<sub>2</sub>Cl<sub>2</sub>. Evaporation of the solvent gave **6** as a green powder (13%): <sup>1</sup>H NMR (800 MHz, DMSO-*d*<sub>6</sub>): δ, ppm: 7.41 (m, 16H), 6.95 (bs, 16H), 3.78 (s, 24H). <sup>13</sup>C NMR (201 MHz, DMSO-*d*<sub>6</sub>) δ, ppm: 159.7, 131.3, 113.9, 55.3. UV/Vis (DMSO) λ<sub>max</sub> nm (log ε) 384 nm (4.91), 597 (4.28), 658 (5.08). HRMS (MALDI) Found: [M]<sup>+</sup> 1393.4336; molecular formula C<sub>80</sub>H<sub>56</sub>MgN<sub>16</sub>O<sub>8</sub> requires [M]<sup>+</sup> 1393.4345.

**Magnesium(II) 2,3,9,10,16,17,23,24-octakis[4-(3,5-bis(benzyloxy)benzyloxy)phenyl]-1,4,8,11,15,18,22,25-(octaaza)phthalocyanine (7)**

Obtained green oil was purified on silica-gel using CH<sub>2</sub>Cl<sub>2</sub> with 1% triethylamine. Collected samples were vaporized and precipitated from CH<sub>2</sub>Cl<sub>2</sub>/CH<sub>3</sub>OH. Formed green solid was subsequently washed with methanol, hexane and acetone to give 32% yield of pure product as green powder. *R*<sub>f</sub> (CH<sub>2</sub>Cl<sub>2</sub>+1% triethylamine) 0.22. <sup>1</sup>H NMR (800 MHz, DMSO-*d*<sub>6</sub>) δ, ppm: 7.79 (bs, 16H), 7.40 (d, J = 7.5 Hz, 32H), 7.34 (t, J = 7.5 Hz, 32H), 7.28 (t, J = 7.5 Hz, 16H), 7.04 (bs, 16H), 6.77 (s, 16H), 6.65 (s, 8H), 5.10 (s, 16H), 5.06 (s, 32H). <sup>13</sup>C NMR (201 MHz, DMSO-*d*<sub>6</sub>) δ, ppm: 159.43, 158.68, 152.98, 149.67, 138.91, 136.65, 131.46, 127.89, 127.82, 127.28, 127.06, 127.00, 114.25, 106.50, 101.42, 69.31, 69.20. UV/Vis (DMSO): λ<sub>max</sub> nm (log ε) 388 nm (5.06), 597 (4.48), 658 (5.32). HRMS (MALDI) Found [M]<sup>+</sup> 3700.4450; molecular formula C<sub>240</sub>H<sub>184</sub>MgN<sub>16</sub>O<sub>24</sub> requires [M]<sup>+</sup> 3700.4267. HPLC purity (see Supplementary data).

**General procedure for synthesis of A<sub>3</sub>B type porphyrazines (8 and 9)**

The magnesium butanol solution was prepared according to the previously described procedure [13]. Magnesium turnings (5 equiv) were refluxed in n-butanol (7 mL for each mmol of substrates) with a catalytic amount of iodine for 3 hours. After cooling down of the slurry, 2,3-dicyanopyrazine derivative (1 equiv) and 1,2-dicyanobenzene (10 equiv) were added and the mixture was refluxed for another 20 hours. After cooling down, reaction mixture was sonicated and filtered through Celite, which was rinsed with toluene and CH<sub>2</sub>Cl<sub>2</sub>. Filtrates were evaporated to dryness giving dark-green, solid residue.

**Magnesium(II) 2,3-bis(4-methoxyphenyl)-1,4-(diazaphthalocyanine (8)**

Obtained product was purified by column chromatography using silica gel and eluents: CH<sub>2</sub>Cl<sub>2</sub>, n-hexane/THF (5:1), CH<sub>2</sub>Cl<sub>2</sub>/MeOH (50:1) to give product as a deep green film (18% yield). *R*<sub>f</sub> (CH<sub>2</sub>Cl<sub>2</sub>/MeOH 35:1) 0.43. <sup>1</sup>H NMR (800 MHz, DMSO-*d*<sub>6</sub>) δ, ppm: 9.38 (m, 4H), 8.24 (m, 4H), 7.90 (m, 6H), 7.17 (m, 6H), 3.96 (s, 3H), 3.95 (s, 3H). <sup>13</sup>C NMR (201 MHz, DMSO-*d*<sub>6</sub>) δ, ppm: 159.6, 155.4, 155.0, 154.0, 152.3, 146.5, 145.7, 138.5, 138.0, 131.4, 131.3, 131.3, 129.8, 129.5, 129.2, 122.5, 122.4, 113.7, 113.6, 55.1, 55.0. UV/Vis (DMSO): λ<sub>max</sub> nm (log ε) 368 nm (4.66), 603 (4.22), 667 (4.95). HRMS (MALDI) Found [M]<sup>+</sup> 750.2125; molecular formula C<sub>44</sub>H<sub>26</sub>MgN<sub>10</sub>O<sub>2</sub> requires [M]<sup>+</sup> 750.2091.

**Magnesium(II) 2,3-bis[4-(3,5-bis(benzyloxy)benzyloxy)phenyl]-1,4-(diazaphthalocyanine (9)**

Obtained product was purified by means of column chromatography using silica gel and eluents: CH<sub>2</sub>Cl<sub>2</sub>, n-hexane/AcOEt (7:2), CH<sub>2</sub>Cl<sub>2</sub>/CH<sub>3</sub>OH (200:1) to give a deep green film (48% yield). *R*<sub>f</sub> (CH<sub>2</sub>Cl<sub>2</sub>/CH<sub>3</sub>OH 50:1) 0.61. <sup>1</sup>H NMR (800 MHz, DMSO-*d*<sub>6</sub>) δ, ppm: 9.13-8.59 (m, 6H), 8.09-7.93 (m, 6H), 7.89 (m, 4H), 7.47 (m, 8H), 7.41 (m, 8H), 7.35 (m, 4H), 7.22 (m, 4H), 6.81 (m, 4H), 6.69 (m, 2H), 5.18 (s, 4H), 5.13 (s, 8H). <sup>13</sup>C NMR (201 MHz, DMSO-*d*<sub>6</sub>) δ, ppm: 159.6, 158.7, 154.7, 154.4, 153.8, 153.5, 152.4, 152.2, 152.0, 145.8, 145.7, 139.3, 138.5, 138.1, 138.0, 136.9, 132.5, 131.9, 129.4, 129.2, 128.4, 128.4, 128.3, 127.9, 127.7, 127.7, 122.5, 114.6, 106.6, 101.3, 69.4, 69.3. UV/Vis (DMSO): λ<sub>max</sub> nm (log ε) 363 nm (4.37), 604 (4.36), 626 (4.38), 676 (5.07). HRMS (MALDI) Found [M+H]<sup>+</sup> 1327.4710; molecular formula C<sub>84</sub>H<sub>58</sub>MgN<sub>10</sub>O<sub>6</sub>+H<sup>+</sup> requires [M+H]<sup>+</sup> 1327.4469. HPLC purity (see Supplementary data).

**X-ray crystallography**

Reflection intensities for **5b** and **5c** were measured at 130 K with an Oxford Diffraction Xcalibur E diffractometer using MoKα radiation and with an Oxford Diffraction SuperNova diffractometer using hi-flux micro-focus Nova CuKα radiation, respectively. Data were processed with CrysAlis PRO software.<sup>39</sup> The structures were solved by direct methods using SIR2014<sup>40</sup> and refined by full matrix least-squares based on F<sup>2</sup> (SHELXL-2014).<sup>41</sup> C-bound hydrogen atoms were placed at idealized positions. All hydrogen atoms were refined as riding on their carriers with U<sub>iso</sub>(H)=1.2U<sub>eq</sub>(CH, CH<sub>2</sub>).

Crystal data for **5b**: C<sub>32</sub>H<sub>22</sub>N<sub>4</sub>O<sub>2</sub>, M = 494.53 g/mol, monoclinic, space group P2<sub>1</sub>/n, a = 8.2968(3) Å, b = 11.2161(5) Å, c = 27.6291(10) Å, β = 97.453(3)°, V = 2549.38(17) Å<sup>3</sup>, Z = 4, T = 130(2) K, μ(MoKα) = 0.082 mm<sup>-1</sup>, D<sub>calc</sub> = 1.288 g/cm<sup>3</sup>, 14332 reflections measured to θ<sub>max</sub> = 25.35°, 4651 unique (R<sub>int</sub> = 0.0376, R<sub>sigma</sub> = 0.0506). The final R indices for 3332 reflections with I > 2σ(I) and 343 refined parameters are R1 = 0.046, wR2 = 0.086 (R1 = 0.0741, wR2 = 0.0969 for all data)

Crystal data for **5c**: C<sub>60</sub>H<sub>46</sub>N<sub>6</sub>O<sub>6</sub>·2(CH<sub>2</sub>Cl<sub>2</sub>), M = 1088.86 g/mol, monoclinic, space group C2/c, a = 23.8249(7) Å, b = 15.5643(4) Å, c = 16.2565(4) Å, β = 117.473(3)°, V = 5348.4(3) Å<sup>3</sup>, Z = 4, T = 130(2) K, μ(CuKα) = 2.474 mm<sup>-1</sup>, D<sub>calc</sub> = 1.352 g/cm<sup>3</sup>, 12425 reflections measured to θ<sub>max</sub> = 68.25°, 4913 unique (R<sub>int</sub> =

## ARTICLE

## Journal Name

0.0428,  $R_{\text{sigma}} = 0.0398$ ). The final R indices for 4091 reflections with  $I > 2\sigma(I)$  and 344 refined parameters are  $R1 = 0.080$ ,  $wR2 = 0.234$  ( $R1 = 0.0888$ ,  $wR2 = 0.2337$  for all data).

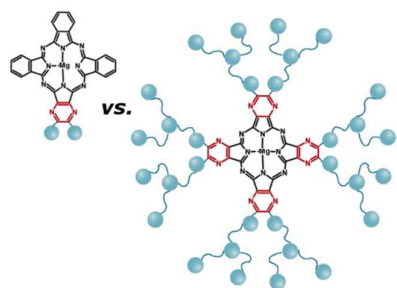
Further details of crystal data collection and structure refinement are given in Table S7 (Supplementary data). Crystallographic data for the structures in this paper have been deposited with the Cambridge Crystallographic Data Centre as supplementary publication CCDC no: 1486351 (for **5b**) and 1486352 (for **5c**). These data can be obtained, free of charge, from The Cambridge Crystallographic Data Centre via [www.ccdc.cam.ac.uk/data\\_request/cif](http://www.ccdc.cam.ac.uk/data_request/cif).

### Acknowledgements

This study was supported by the Polish National Science Centre under Grant No. 2012/05/E/NZ7/01204. SJ and LP acknowledge financial support from the National Centre for Research and Development, contract number PBS1/A9/13/2012.

### References

- M. S. Rodríguez-Morgade and P. A. Stuzhin, *J. Porphyr. Phthalocyanines*, 2004, **8**, 1129–1165.
- D. Wöhrle, G. Schnurpfeil, S. G. Makarov, A. Kazarin and O. N. Suvorova, *Macroheterocycles*, 2012, **5**, 191–202.
- M. G. Vicente, *Curr. Med. Chem. Anti-Cancer Agents*, 2001, **1**, 175–194.
- G. de la Torre, C. G. Claessens and T. Torres, *Chem. Commun. Camb. Engl.*, 2007, 2000–2015.
- J. a. a. W. Elemans, R. van Hameren, R. J. M. Nolte and A. E. Rowan, *Adv. Mater.*, 2006, **18**, 1251–1266.
- M. P. Donzello, C. Ercolani, V. Novakova, P. Zimcik and P. A. Stuzhin, *Coord. Chem. Rev.*, 2016, **309**, 107–179.
- V. N. Nemykin and E. A. Lukyanets, *Arkivoc*, 2010, **1**, 136–208.
- A. B. Ormond and H. S. Freeman, *Materials*, 2013, **6**, 817–840.
- A. E. O'Connor, W. M. Gallagher and A. T. Byrne, *Photochem. Photobiol.*, 2009, **85**, 1053–1074.
- D. I. Rosenthal, P. Nurenberg, C. R. Becerra, E. P. Frenkel, D. P. Carbone, B. L. Lum, R. Miller, J. Engel, S. Young, D. Miles and M. F. Renschler, *Am. Assoc. Cancer Res.*, 1999, **5**, 739–745.
- J.-Y. Jaung, *Dyes Pigments*, 2007, **75**, 420–425.
- C. K. Jang and J. Y. Jaung, *Mater. Lett.*, 2008, **62**, 3209–3212.
- R. P. Linstead and M. Whalley, *J. Chem. Soc. Resumed*, 1952, 4839–4846.
- E. Wiczorek, M. Gierszewski, L. Popenda, E. Tykarska, M. Gdaniec, S. Jurga, M. Sikorski, J. Mielcarek, J. Piskorz and T. Goslinski, *J. Mol. Struct.*, 2016, **1110**, 208–214.
- R. Cristiano, E. Westphal, I. H. Bechtold, A. J. Bortoluzzi and H. Gallardo, *Tetrahedron*, 2007, **63**, 2851–2858.
- B. H. Lee, J. Y. Jaung, S. C. Jang and S. C. Yi, *Dyes Pigments*, 2005, **65**, 159–167.
- T. Goslinski, J. Piskorz, D. Brudnicki, A. J. P. White, M. Gdaniec, W. Szczolko and E. Tykarska, *Polyhedron*, 2011, **30**, 1004–1011.
- J. Piskorz, E. Tykarska, M. Gdaniec, T. Goslinski and J. Mielcarek, *Inorg. Chem. Commun.*, 2012, **20**, 13–17.
- W. Szczolko, L. Sobotta, P. Fita, T. Koczorowski, M. Mikus, M. Gdaniec, A. Orzechowska, K. Burda, S. Sobiak, M. Wierzchowski, J. Mielcarek, E. Tykarska and T. Goslinski, *Tetrahedron Lett.*, 2012, **53**, 2040–2044.
- M. Kryjewski, E. Tykarska, T. Rebis, J. Długaszewska, M. Ratajczak, A. Teubert, J. Gapiński, A. Patkowski, J. Piskorz, G. Milczarek, M. Gdaniec, T. Goslinski and J. Mielcarek, *Polyhedron*, 2015, **98**, 217–223.
- V. Novakova, M. Lásková, H. Vavříčková and P. Zimcik, *Chem. – Eur. J.*, 2015, **21**, 14382–14392.
- V. Novakova, M. Miletin, K. Kopecky and P. Zimcik, *Chem. – Eur. J.*, 2011, **17**, 14273–14282.
- M. Machacek, J. Demuth, P. Cermak, M. Vavreckova, L. Hruba, A. Jedlickova, P. Kubat, T. Simůnek, V. Novakova and P. Zimcik, *J. Med. Chem.*, 2016.
- P. Secondo and F. Fages, *Org. Lett.*, 2006, **8**, 1311–1314.
- J. Zhu, R. Beugelmans, S. Bourdet, J. Chastanet and G. Roussi, *J. Org. Chem.*, 1995, **60**, 6389–6396.
- K. Thakkar, R. L. Geahlen and M. Cushman, *J. Med. Chem.*, 1993, **36**, 2950–2955.
- V. Percec, M. Peterca, M. J. Sienkowska, M. A. Ilies, E. Aqad, J. Smidrkal and P. A. Heiney, *J. Am. Chem. Soc.*, 2006, **128**, 3324–3334.
- N. M. Loim and E. S. Kelbysheva, *Russ. Chem. Bull.*, 2004, **53**, 2080–2085.
- C. J. Hawker and J. M. J. Frechet, *J. Am. Chem. Soc.*, 1990, **112**, 7638–7647.
- T. P. Forsyth, D. B. G. Williams, A. G. Montalban, C. L. Stern, A. G. M. Barrett and B. M. Hoffman, *J. Org. Chem.*, 1998, **63**, 331–336.
- M. Brewis and G. J. Clarkson, *Chem. Commun.*, 1998, 969–970.
- E. H. Mørkved, N. K. Afseth and P. Zimcik, *J. Porphyr. Phthalocyanines*, 2007, **11**, 130–138.
- J. Mack and N. Kobayashi, *Chem. Rev.*, 2011, **111**, 281–321.
- A. Ogunsipe, D. Maree and T. Nyokong, *J. Mol. Struct.*, 2003, **650**, 131–140.
- T. Goslinski, T. Osmalek and J. Mielcarek, *Polyhedron*, 2009, **28**, 3839–3843.
- I. Seotsanyana-Mokhosi, N. Kuznetsova and T. Nyokong, *J. Photochem. Photobiol. A*, 2001, **140**, 215–222.
- W. Spiller, H. Kliesch, D. Woehrle, S. Hackbarth, B. Roeder and G. Schnurpfeil, *J. Porphyr. Phthalocyanines*, 1998, **2**, 145–158.
- A. Tillo, M. Stolarska, M. Kryjewski, L. Popenda, L. Sobotta, S. Jurga, J. Mielcarek and T. Goslinski, *Dyes Pigments*, 2016, **127**, 110–115.
- Agilent Technologies, CrysAlis PRO software; Agilent Technologies: Yarnton, Oxfordshire, England, 2011.*
- M. C. Burla, R. Caliandro, M. Camalli, B. Carrozzini, G. L. Cascarano, L. De Caro, C. Giacovazzo, G. Polidori and R. Spagna, *J. Appl. Crystallogr.*, 2005, **38**, 381–388.
- G. M. Sheldrick, *Acta Crystallogr. Sect. C Struct. Chem.*, 2015, **71**, 3–8.



- Singlet oxygen generation yields and aggregation tendencies were studied for porphyrazines bearing dendrimeric substituents.